p INVERSION LAYER SI SOLAR CELLS AS TEST FOR THE I¯S STRUCTURE: RESULTS AND PROSPECTS

D. König [1], D.R.T. Zahn [1], R. Reich [2], K. Gottfried [2], G. Ebest [2],
[1] Institut für Physik, TU Chemnitz, Germany [2] Zentrum für Mikrotechnologien, TU Chemnitz, Germany

ABSTRACT

The I¯S structure is a novel layer arrangement serving as a source for a negative drift field. Its application to solar cells is manifold and does *not* depend on Si. The deposition of the Aluminium Fluoride (AlF_3) layer involved can be implemented as final process in solar cell production; thus compatibility to existing processing sequences is given. First prototypes of a p inversion layer solar cell on Si were prepared providing evidence of function for the I¯S structure. While conditions of preparation were far from optimum, a relative increase in conversion efficiency of 21 % was achieved for solar cells with I¯S structure versa solar cells without it. For testing the field effect impact the AlF_3 layer thickness was chosen to be 15 nm thus eliminating its additional advantage as anti-reflective coating (ARC).

1. INTRODUCTION

The I¯S structure consists of a layer stack AlF_3 / SiO_2 on a semiconductor as e.g. Si (Fig. 1) [1].

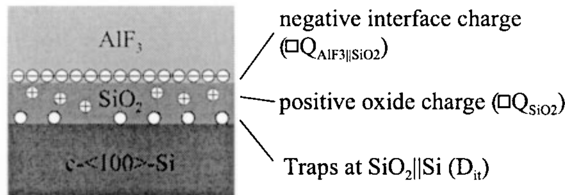

Figure 1: I¯S structure with Si substrate.

p inversion layer solar cells (p-ILSCs) based on an n-Si substrate are adequate test devices for the I¯S structure due to the floating p/n junction induced by the negative charge (Fig. 2).

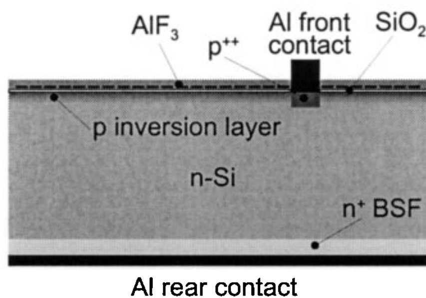

Figure 2: Composition of p inversion layer solar cell.

The I¯S structure has an effective charge (average of 49 point wafer map over entire sample) of typically $\square N_{eff} = -4 \times 10^{12}\,\mathrm{cm}^{-2}$ [2]; peak values were in the range of $\square N_{eff} = -6.9 \times 10^{12}\,\mathrm{cm}^{-2}$ [3]. The negative charge is $\square Q_{AlF_3||SiO_2} = -1.0 \ldots -2.0 \times 10^{13}\,\mathrm{cm}^{-2}$ and is located at the interface $AlF_3||SiO_2$. A positive charge of the SiO_2 layer is typically $\square Q_{SiO_2} = 4 \times 10^{11}\,\mathrm{cm}^{-2}$. The effective surface recombination velocity of Float Zone (FZ) - p-Si wafers dropped from $S_{eff} = 2360\,\mathrm{cms}^{-1}$ for samples with a Rapid Thermal Oxide (RTO) of $d_{SiO_2} = 1.6\,\mathrm{nm}$ to $S_{eff} = 173\,\mathrm{cms}^{-1}$ for samples with RTO of same thickness and an additional AlF_3 layer of thickness $d_{AlF_3} = 20\,\mathrm{nm}$ [3]. Values of S_{eff} on FZ - n-Si wafers are expected to be significantly lower due to formation of a p inversion layer.

2. PREPARATION AND TECHNOLOGY

The preparation of the p-ILSC requires the modification of common process sequences. As substrate 4" c-Si wafers with $N_D = 5 \times 10^{15}\,\mathrm{cm}^{-3}$ were used. The following list shows the outline of preparation; novel/modified processes are written in *italics*:

1. cleaning (RCA process)
2. spin on of Phosphorous - Spin On Dope (P-SOD) on rear side
3. *Rapid Thermal Diffusion (RTD) for n^+ BSF with in situ gettering of outdiffusing P*
4. PVD of Aluminum (Al) layer on front side
5. photo lithography and etch of Al (finger grid)
6. *RTO (areas not covered with Al) and RTD (p^+ area underneath contact grid) in situ*
7. etch back of P-SOD on rear side (front side covered with laquer)
8. H_2 passivation
9. evaporation of Al on rear side (rear contact)
10. *Physival Vapour Deposition (PVD) of 15 nm AlF_3 onto front side using hard mask (only cell areas covered with AlF_3)*

Process 3 is modified by adding HCl to the process gas usually employed (pure N_2). The HCl gas reacts with P outdiffusing from the P-SOD [3]:

$$P_2O_5 + 6\,HCl \longrightarrow 2\,POCl_3 + 3\,H_2O \qquad (1)$$

Both products of the chemical reaction – Phosphorylchloride and Water – are gaseous and get pumped off from the RTP reactor. Thereby a contamination of the RTP reactor with P is prevented [3].

Underneath the contact grid a p^+ area is needed. On the other hand, a passiviating RTO layer is needed on the pure Si surface. Exposing the Al finger grid to Oxygen (O_2) results in an Alumina (Al_2O_3) layer which helps to keep the finger grid in its original shape during RTP. Thus an *in situ* RTD - RTO becomes feasible, thereby saving one RTP step. The shape of the finger grid only changes gradually. An optimization of Al reflow during the *in situ* RTD - RTO can be made in advance by redesigning the grid layout [3].

Finally, the PVD of the AlF_3 layer presents a novel process. However, its deposition resembles that of MgF_2 which is common standard as ARC on solar cells. The PVD has to be modified only such that a Fluorine (F) deficiency is accomplished at the interface $AlF_3 || SiO_2$ [3, 4, 5]. The PVD process has got a thermal budget which is roughly as much as needed for forming a 1.5 nm RTO on Si; the deposition time is within the range of $t = 20 \ldots 300$ s. Since the PVD of AlF_3 is carried out as the final process its integration into an existing colar cell manufacture is rather trivial; the problem of F contamination does not occur. During PVD F atoms are passivating the SiO_2 surface, saturating Si dangling bonds [3]. The bond energy Si—F exceeds the bond energy Si—H by a factor of 47 [6], resulting in a much more robust passivation of traps in the vicinity of the SiO_2 surface.

Four wafers (samples 81/5 ... 81/8) with six p-ILSCs each were prepared in the same way. Fig. 3 shows a wafer with prototypes. The thin AlF_3 layer can be seen as faint shade around the contact grids. Its field impact sets up the edge of the p-ILSC as without negative charge there is no p/n floating junction.

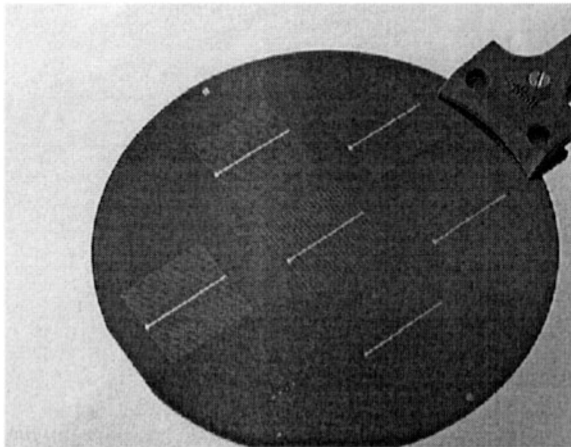

Figure 3: Prototypes of p-inversion layer solar cells with $A = 4\,\mathrm{cm}^2$ each. AlF_3 coating, $d_{AlF_3} = 15$ nm, can be seen as a faint shade around grids.

Sample 81/5 was without AlF_3 layer served as a reference sample. Each cell possesses a total area of $A = 4\,\mathrm{cm}^2$. The contact grid layout of cell 1 is equivalent to cell 4 as cell 2 is equivalent to cell 3. Therefore only the data of the cells 3 ... 6 are presented here. The thickness of the Al layer forming the contact grid has been 4 μm. Each cell has got a bus bar which is 300 μm wide and ends in a contact pad of $600 \times 1000\,\mu\mathrm{m}^2$. Table 1 shows the dimensions of the respective contact grids.

Table 1: Finger width w_f, finger distance d_f and relative share ϕ_{gr} of contact grid on the total cell area A depending on contact grid layout (solar cell type).

cell type	w_f / μm	d_f / μm	ϕ_{gr} / % A_{cell}
3	20	505	5.44
4	20	979	3.67
5	20	405	6.3
6	30	495	7.36

2.1 Conditions of preparation

Fig. 4 shows the SIMS profile of a control wafer processed with the prototypes apart from metallization and PVD of AlF_3.

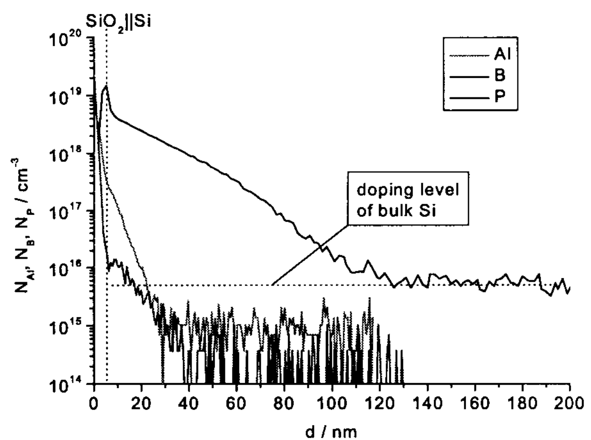

Figure 4: SIMS profile of control wafer processed with the prototypes apart from metallization and PVD of AlF_3.

With the concentration of donors in the vicinity of the Si surface being so high a massive screening of the external negative charge occurs.

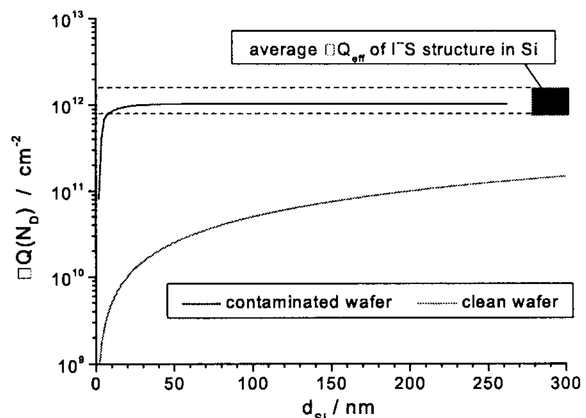

Figure 5: Negative charge sheet density in Si induced by P for the sample of Fig. 4 and for a clean wafer with constant doping density of $N_D = 5 \times 10^{15}\,\mathrm{cm}^{-3}$.

Fig. 5 shows the calculated surface charge of ionized donors calculated by integrating the P volume density over the sample depth. The external negative charge is shown; its value in Si is lower due to ε_{Si} which is higher than ε of the insulators. Obviously the external negative charge is compensated after $d_{Si} \approx 30\,\mathrm{nm}$ so that a significant p inversion layer cannot exist. The impact of the negative charge is limited to the passivation of the Si surface what is useful for passivating an n^+ conduction layer of a conventional solar cell. However, this had not been the goal.

Although the conditions of preparation were very far from optimum (Figs. 4 and 5, next paragraph) an increase in conversion efficiency η was achieved on all samples with AlF_3 layer (see section 2.2). The layer thickness of AlF_3 had been chosen to 15 nm, thus ruling out any optical advantage (ARC) of the samples with AlF_3 layer over the reference samples.

Due to a very short period of two weeks at which the required process equipment had been available an optimization of the process sequence could not be carried out. This refers especially to the *in situ* RTD-RTO. However, the major obstacle had been the massive pollution of the RTP reactor with P *prior* to the processing of p-ILSCs. While P can be gettered *in situ* (process 3, eq. 1) at the RTD, there is no chance to do so if Al is present at the *in situ* RTD-RTO. Al would react fiercely with HCl to form $AlCl_3$ and H_2, removing any Al from the wafer surface.

2.2 Results

Fig. 6 shows the dark current density $\vec{J}$ over bias voltage V of the cells with grid type 3. It is obvious that the J/V characteristics are far from optimum.

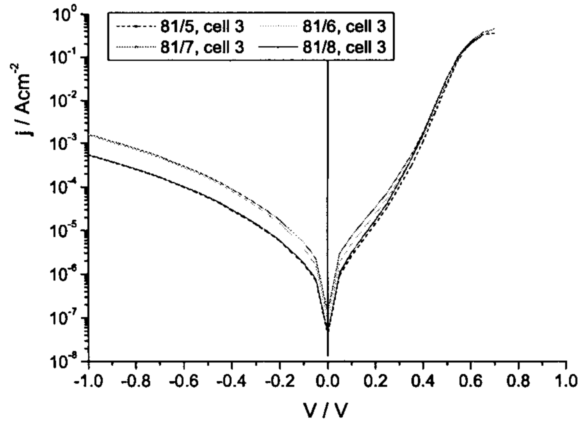

Figure 6: Dark J/V characteristics of cells, grid type 3. Reference cell is 81/5-3, other cells are from different wafers (6, 7, 8).

As an optimization of the *in situ* RTD-RTO could not be carried out an optimal p/n junction underneath the contact grid cannot be expected. Another reason is the indiffusion of P at the edge of the p^+ region leading to a very high recombination rate due to the massive presence of acceptors and donors.

With the dark J/V characteristics being far from optimum the active J/V curves are shifted towards the passive operating area of the cells, resulting in a low open circuit voltage of and a very low short circuit current density. Fig. 7 shows the active J/V curves of the solar cells with grid type 3; the relevant data are listed in Table 2.

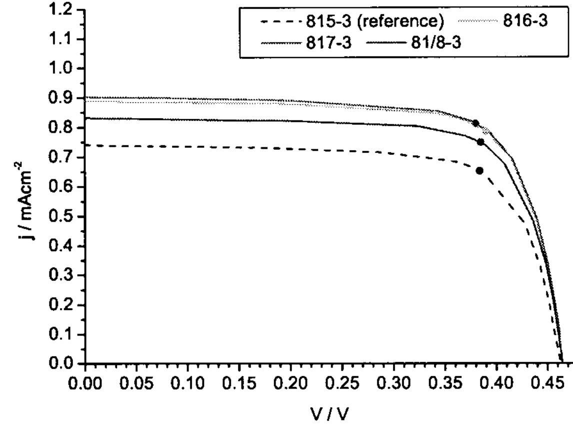

Figure 7: Active J/V curves of cells, grid type 3. Dots denote MPPs.

Table 2: Active J/V data of cell 3 for all samples.

Probe	81/5	81/6	81/7	81/8
V_{OC} /V	0.462	0.463	0.462	0.462
$\vec{j}_{SC}$ /mAcm^{-2}	0.742	0.889	0.903	0.832
V_{MPP} /V	0.383	0.390	0.380	0.385
$\vec{j}_{MPP}$ /mAcm^{-2}	0.653	0.786	0.812	0.748
η /%	0.250	0.307	0.309	0.288
FF /%	72.9	74.2	73.7	74.4

Fig. 8 depicts the density of extracted power P_{MPP} from all cell types.

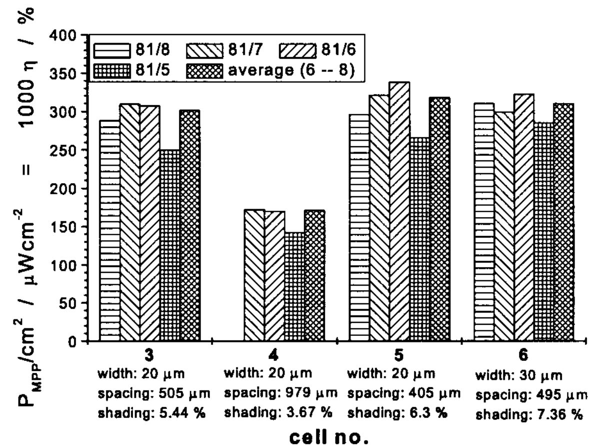

Figure 8: Power density at MPP of cells 3 ... 6. Cells of sample 81/5 serve as reference. The average for each cell of samples 81/6 ... 8 is also shown. Legend: cell number, finger width, finger distance, relative share of contact grid on total cell area.

The cells were illuminated with light having the equivalent intensity and spectral distribution of 1 Sun and AM 1.5, respectively. This corresponds to a power density of $1\,\mathrm{kWm}^{-2}$. In Fig. 8 P_{MPP} is given in $\mu\mathrm{Wcm}^{-2}$ with $P_{MPP} = 100\,\mu\mathrm{Wcm}^{-2}$ being equivalent to $\eta = 0.1\,\%$.

Fig. 8 shows that all cells with $I^{-}S$ structure possess an increased η referring to the reference cells. For the cell types 3, 5 and 6 η is 21 % relative above the reference cells of sample 81/5. The cell type 4 presents an exception as the finger distance and thus the average diffusion path of holes to the p^{+} contacts is roughly twice as large as for the other cell types. Due to the suppressed formation of a significant p inversion layer mentioned above the collection probability for holes is therefore reduced even further, resulting in η being 17 % relative above the reference cell. With uncontaminated RTP equipment and optimized RTP processing conversion efficiencies within the range of n inversion layer solar cells are feasible.

Using the AlF_3 layer as an ARC causes η to increase further. However, for prooving the field impact of the $I^{-}S$ structure, the layer thickness had been chosen not to meet the requirements of an ARC. Thereby the increased η can be assigned to the field impact unambiguously.

3. APPLICATIONS & PROSPECTS

The most obvious application of the $I^{-}S$ structure is the generation of a p inversion layer as applied on the prototypes mentioned above. An enhanced surface passivation of n^{+} layers underneath the front surface of conventional solar cells can be accomplished by inducing an n depletion zone. Thus the free carrier product $n \times p$ is decreased, resulting in a better Blue Response of the cells. For selective rear contact cells a field supporting the p^{+} BSF can be introduced. Thereby the doping density of the BSF can be decreased. In principle the $I^{-}S$ structure can be realized with any semiconductor if the band offsets stay in a favourable range [3]. For that reason there is a broad range of materials to be tested. Additionally, all applications mentioned can exploit the optical properties of AlF_3 for an ARC.

On a long term perspective the application on Quantum Well Solar Cells (QWSCs) seems to be a promising goal. QWSCs consist of ultrathin layers being stacked upon each other. Highly doped regions as field sources for carrier separation will not be feasible anymore without degrading the quantum wells for thermodynamical reasons of semiconductor doping [3]. Processes for monolayer deposition of doped semiconductors like Molecular Beam Epitaxy are unable to meet the requirements for large scale production. By using two antipolar external field sources with fixed charges both carrier separation and surface passivation can be achieved. For promoting carrier tunneling through the external field sources these insulator layers have to be very thin. As the F deficiency needed for building up a fixed negative charge is an interface effect, the AlF_3 layer can be sufficiently thin for tunneling transport without its fixed negative charge density being decreased [3].

4. CONCLUSIONS

First prototypes of p inversion layer silicon solar cells were prepared as test devices for the $I^{-}S$ structure. Although an optimization of the novel process sequence could not be carried out and conditions of preparation were far from optimum an increase in efficiency by the $I^{-}S$ structure was achieved on all samples.

A brief discussion of possible applications showed the great potential of the $I^{-}S$ structure for increasing conversion efficiencies on different solar cell topologies. On a long term perspective the usage at Quantum Well Solar Cells (QWSCs) is very promising as the conventional method of field implementation by doping will fail on such ultrathin layer arrangements.

Acknowledgements

The author wishes to thank the Foundation For The Promotion Of German Sciences (Stiftung zur Förderung der deutschen Wissenschaften) for financial support and the German Research Foundation (DFG) for a post graduate research fellowship.

REFERENCES

[1] D. König, G. Ebest, Solid State Electron. **44**, 111 (2000)

[2] D. König, R. Scholz, S. Gemming, I. Thurzo, T.U. Kampen, D.R.T. Zahn, G. Ebest, Physica E **14**, 259 (2002)

[3] D. König, Isolatorschichtanordnungen mit negativen Festladungen und ihre Anwendung an Silicium-Solarzellen, PhD thesis, Institute of Physics, TU Chemnitz, Febr. 2003

[4] D. König, G. Ebest, Solar Energy Mater. Solar Cells **75**, 335 (2003)

[5] D. König, K. König: Solar Cell Surface, International Patent (PCT), Publ. No. WO 02/41408 A1, 16th Nov. 2001

[6] A. F. Holleman, N. Wiberg, *Lehrbuch der anorganischen Chemie*, 101st Ed., Walter de Gruyter, Berlin, 1995